

Biomechanical Prediction of Veins and Soft Tissues beneath Compression Stockings Using Fluid-Solid Interaction Model

Chongyang Ye, Rong Liu

Abstract—Elastic compression stockings (ECSs) have been widely applied in prophylaxis and treatment of chronic venous insufficiency of lower extremities. The medical function of ECS is to improve venous return and increase muscular pumping action to facilitate blood circulation, which is largely determined by the complex interaction between the ECS and lower limb tissues. Understanding the mechanical transmission of ECS along the skin surface, deeper tissues, and vascular system is essential to assess the effectiveness of the ECSs. In this study, a three-dimensional (3D) finite element (FE) model of the leg-ECS system integrated with a 3D fluid-solid interaction (FSI) model of the leg-vein system was constructed to analyze the biomechanical properties of veins and soft tissues under different ECS compression. The Magnetic Resonance Imaging (MRI) of the human leg was divided into three regions, including soft tissues, bones (tibia and fibula) and veins (peroneal vein, great saphenous vein, and small saphenous vein). The ECSs with pressure ranges from 15 to 26 mmHg (Classes I and II) were adopted in the developed FE-FSI model. The soft tissue was assumed as a Neo-Hookean hyperelastic model with the fixed bones, and the ECSs were regarded as an orthotropic elastic shell. The interfacial pressure and stress transmission were simulated by the FE model, and venous hemodynamics properties were simulated by the FSI model. The experimental validation indicated that the simulated interfacial pressure distributions were in accordance with the pressure measurement results. The developed model can be used to predict interfacial pressure, stress transmission, and venous hemodynamics exerted by ECSs and optimize the structure and materials properties of ECSs design, thus improving the efficiency of compression therapy.

Keywords—Elastic compression stockings, fluid-solid interaction, tissue and vein properties, prediction.

I. INTRODUCTION

ECSs have been applied as a valid auxiliary modality for prevention or treatment of chronic venous disorders such as deep venous thrombosis, post-thrombotic syndrome, and leg ulceration through improving venous return, calf muscular pumping action and control of lymphedema [1]-[4]. The medical function of ECSs is to oppose the increased venous hypertension by decreasing the luminal diameter and increasing the flow velocity [5]. The maximum pressure is exerted at the distal and decreasing up to the proximal leg. The medical treatment effectiveness largely depends on the interfacial

pressure distributions and internal stress transmission [6].

To increase the precautionary and therapeutic effects, appropriate measurement and evaluation of the magnitudes and distributions of the applied interfacial pressure are essential. Currently, three main methods are applied to obtain interfacial pressure. They are direct measurements by using pressure sensors [7], pressure calculation based on Laplace's Law [8], [9], and FE model for pressure prediction [10]. However, stress transmission from the skin to the soft tissue within the lower limb cannot be predicted by Laplace's Law and be determined by direct measurement using pressure sensors [7], [8], whereas stress transmission largely determines the pressure function of ECSs, which reflects the effectiveness of the mechanical forces applied to the venous walls.

Previous studies applied a zero-dimensional or one-dimensional model to predict venous hemodynamic properties [11]. However, these existing models did not take the effects of soft tissue and venous position into account. Moreover, few studies addressed [11]-[14] the essential question on the venous hemodynamic properties including flow velocity and wall shear stress of 3D leg model. In this study, therefore a 3D biomechanical FE model for numerically simulating the interfacial pressure and stress transmission and a FSI model for analyzing venous hemodynamics was constructed based on the MRI scanning images and digital analysis technologies. This technique will provide a method to assess the interfacial pressure, stress transmission, and venous flow under the action of ECSs with different pressure classes and enhance our understanding of the dynamic interaction between ECSs and lower limb with reasonable accuracy.

II. METHODOLOGY FOR FE MODEL

A. Health Screening and 3D Digital Body Scanning

3D leg model with precise and reproducible capture (point density: 200 points/cm³ scan time: 6-10 s) was developed. The dimensions of the bare right lower limb at the key anatomic regions were recorded for 3D digital modeling.

B. Reconstruction of Geometries of Subject-Specific Lower Limb and ECSs

The geometry of the subject's right lower limb was reconstructed from coronal images via MRI scanning. The MR image slices in thickness of 1.5 mm and an in-plane voxel size of 0.98 mm × 0.98 mm were taken when the subject was supine and fixed by a specially made leg brace. In this FE model, the

R Liu is with the Institute of Textiles and Clothing, The Hong Kong Polytechnic University, Hong Kong SAR, China (corresponding author, phone: (852) 2766-6473; fax: (852) 2773-1432; e-mail: rong.liu@polyu.edu.hk).

CY Ye is with the Institute of Textiles and Clothing, The Hong Kong Polytechnic University, Hong Kong SAR, China (e-mail: y14489274@163.com).

soft tissues (skin and muscle) and the bones (femur, patella, fibula and tibia) were constructed by using Mimics (v20.0) software. The SCDM (v19.2, ANSYS, Inc.) skin surface tool was applied in sketching and creating patches on the facets and stitching the patches together to form a continuous body and to determine the faces.

The geometry and three graduation zones of ECS was reconstructed using the FE Package ANSYS Workbench (v19.2, ANSYS, Inc.) according to the size and shape of our developed ECS samples.

C. Biomechanical Interaction between Lower Limb and ECSs

In the process of the wearing, ECS is stretched along the lower limb to exert pressure to the leg surface, resulting in deformation of limb tissue. Laplace's Law was employed to analyze the relations between ECS material properties and interfacial pressure, which is expressed as [8]:

$$P = \frac{T}{R}$$

where P is the contact pressure, T is the tension of elastic materials and R is the radius of lower limb. However, this formula is not suitable to determine the interfacial pressure value. Proper contact setting and frictional contact should be involved in the FE model to impede element penetrations.

D. Determination of the Material Properties

The ECSs are assumed as a homogeneous, orthotropic and linear elastic material. Young's modulus, Poisson's Ratio, and shear modulus were determined in our model through applying INSTRON and Kawabata KES-FB1 assessment, respectively, under a standard ISO13934-1:1999 testing condition (20 ± 2 °C temperature, $65 \pm 4\%$ relative humidity) (Tables I-III).

The soft tissue is assumed as homogeneous, isotropic, quasi-incompressible, which can be governed by a Neo-Hookean strain energy density function

$$W = C_1 (\bar{I}_1 - 3) + D_1 (J - 3)^2 \quad (1)$$

where W is strain energy density function, and C_1 and D_1 are 5000 Pa and 1.4×10^{-7} Pa⁻¹, respectively [15]. I_1 is the first invariant of the Cauchy-Green deformation tensor and J is the volume ratio. For consistency with linear elastic, C_1 and D_1 can be expressed as,

$$C_1 = \frac{\mu}{2}, D_1 = \frac{\lambda}{2} \quad (2)$$

where C_1 and D_1 are shear modulus and bulk modulus, respectively. The C_1 and D_1 of the soft tissue are 0.005 MPa and 7.14 MPa, respectively.

E. Meshing and Boundary Conditions of FE Model

The ECSs shell and lower limbs were meshed using linear

Tetrahedrons elements under ANSYS Workbench (v19.2) modeling environment. Their total nodes and elements are approximately 50000 and 200000, respectively. The mesh quality was about 0.85, indicating a perfect cube in our elements (Fig. 1). The tibia and fibula were fixed in the FE model and 340 mm deformation loading of ECS was adopted in our model.

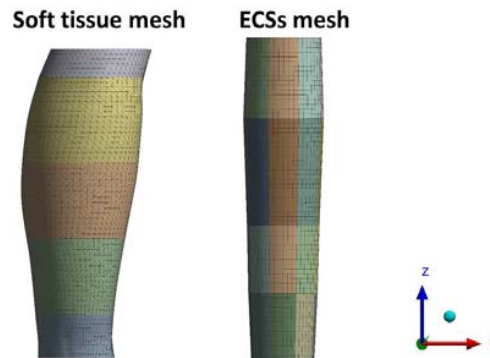


Fig. 1 Meshing for the soft tissue and ECS

F. Pressure Validation

The interfacial pressures between the ECSs and the lower limb were measured *in vivo* by using a pneumatic pressure transducer to validate the developed subject-specific FE model. A total of 12 typical sites at the ankle, brachial and calf and around anterior, posterior, medial and lateral leg was tested when the subject was being in standing position and worn with the tailor-made ECSs.

III. METHODOLOGY FOR FSI MODEL

A. Reconstruction of Geometries of Veins and Soft Tissue

The geometry of peroneal vein, small saphenous vein, and great saphenous vein of the lower limb was reconstructed from the coronal images via MRI scanning. The spatial position of veins was based on MRI images, and the cross-section of veins was processed with smooth treatment as a circle since the fewer pixels induced irregular vein surface (Fig. 2).

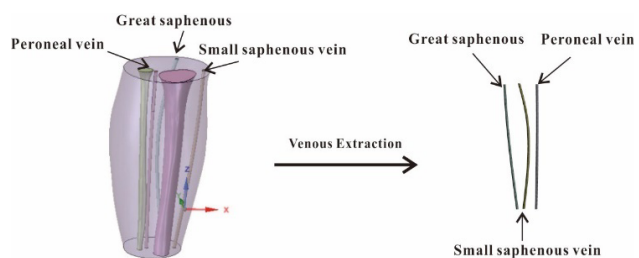


Fig. 2 Reconstruction of the lower limb and the veins

B. Venous Flow Analysis

The Reynolds number (Re) is an important dimensionless quantity in fluid mechanics that is used to predict flow patterns in different fluid flow situations, which can be defined as,

$$Re = \frac{\rho v L}{\mu} \quad (3)$$

where ρ is the density of veins, and v and μ denote flow velocity and dynamic viscosity of veins, respectively, and L is the length of the vein. Re of veins was less than 2300, the flow of veins was regarded as laminar flow, which means that the direction of venous flow parallels to the venous wall. The venous flow moves in a straight line parallel to the venous wall without eddies and swirls.

Navier-Stokes equation was used to analyze venous hemodynamic properties including velocity and pressure. The venous flow can be assumed to be Poiseuille flow, which is the steady flow of an incompressible fluid parallel to the axis of a circular pipe of infinite length. The venous center is moving fastest while the venous wall is stationary with no-slip condition based on Poiseuille flow assumption. Navier-Stokes equation can be simplified as:

$$\frac{dp}{dx} = \mu \frac{d^2 u}{dy^2} \quad (4)$$

C. Meshing for FSI Model

The vein models were meshed using fluent tetrahedron elements with boundary layer (Fig. 3). The total elements were approximately 75000 in the vein model. Dynamic mesh was applied in the FSI model through smoothing, layering and remeshing methods. The thickness of the dynamic mesh was set as 0.1 mm.

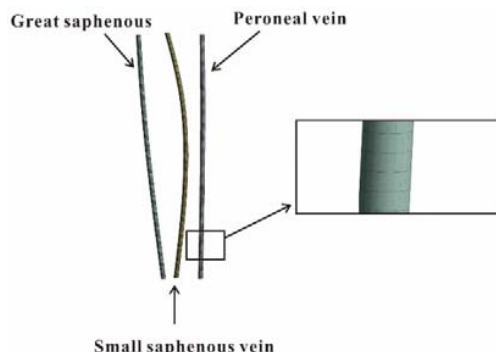


Fig. 3 Meshing for the veins

D. Boundary Conditions

The velocity inlet (v_{inlet}) and the pressure outlet (P_{outlet}) were set in our model. The velocity inlet was set at 0.1 m/s [16], and the pressure outlet was set at 0 Pa, which means that the veins can be regarded as a free outflow. The external pressure exerted by Class-I ECS on the skin surface was applied.

E. FSI Model Solution

A coupling system combining the Static structure and Fluent with steady solution were developed in our FSI model. The venous walls were defined as a solid-fluid interaction interface. The time step of FSI coupling system was set as 5, and the iteration number of Fluent was set as 2000.

IV. RESULTS

A. ECSs Mechanical Properties

The ECSs mechanical properties were shown in Table I. The Young's moduli around the cross-section of the ankle were approximately 0.35 MPa, 0.47 MPa and 0.55 MPa for Types I, II, and III, respectively, of the ECSs with pressure Classes I and II. Correspondingly, the longitudinal Young's moduli along the ankle region were approximately 0.21 MPa, 0.27 MPa and 0.31 MPa, respectively. The cross-sectional and longitudinal Young's moduli at the calf and knee were slightly lower than those at the ankle. The Poisson's ratios of our ECS samples were approximately 0.28 (Table II). The cross-sectional shear modulus of Class-I-Type I-ECS at ankle was 0.14 MPa, which was approximately 40% of the cross-sectional Young's modulus of Class-I-Type-I-ECS at the same section.

TABLE I
YOUNG'S MODULI FOR ECSs

| E (MPa) | Ankle | Calf | Knee |
|---------------------------|-------|------|------|
| E_x (class I-Type I) | 0.35 | 0.20 | 0.14 |
| E_y (class I-Type I) | 0.35 | 0.20 | 0.14 |
| E_z (class I-Type I) | 0.21 | 0.13 | 0.09 |
| E_x (class I-Type II) | 0.47 | 0.27 | 0.17 |
| E_y (class I-Type II) | 0.47 | 0.27 | 0.17 |
| E_z (class I-Type II) | 0.27 | 0.15 | 0.10 |
| E_x (class II-Type III) | 0.55 | 0.36 | 0.21 |
| E_y (class II-Type III) | 0.55 | 0.36 | 0.21 |
| E_z (class II-Type III) | 0.31 | 0.21 | 0.14 |

TABLE II
POISSON'S RATIOS FOR ECSs

| ν | Ankle | Calf | Knee |
|--------------------------------|-------|------|------|
| ν_{xy} (class I-Type I) | 0.26 | 0.28 | 0.29 |
| ν_{xz} (class I-Type I) | 0.26 | 0.28 | 0.29 |
| ν_{yz} (class I-Type I) | 0.26 | 0.28 | 0.29 |
| ν_{xy} (class I-Type II) | 0.26 | 0.28 | 0.29 |
| ν_{xz} (class I-Type II) | 0.26 | 0.28 | 0.29 |
| ν_{yz} (class I-Type II) | 0.26 | 0.28 | 0.29 |
| ν_{xy} (class II-Type III) | 0.26 | 0.28 | 0.29 |
| ν_{xz} (class II-Type III) | 0.26 | 0.28 | 0.29 |
| ν_{yz} (class II-Type III) | 0.26 | 0.28 | 0.29 |

TABLE III
SHEAR MODULI FOR ECSs

| G (MPa) | Ankle | Calf | Knee |
|------------------------------|-------|------|------|
| G_{xy} (class I-Type I) | 0.14 | 0.08 | 0.05 |
| G_{xz} (class I-Type I) | 0.08 | 0.05 | 0.03 |
| G_{yz} (class I-Type I) | 0.08 | 0.05 | 0.03 |
| G_{xy} (class I-Type II) | 0.19 | 0.11 | 0.07 |
| G_{xz} (class I-Type II) | 0.11 | 0.06 | 0.04 |
| G_{yz} (class I-Type II) | 0.11 | 0.06 | 0.04 |
| G_{xy} (class II-Type III) | 0.22 | 0.14 | 0.09 |
| G_{xz} (class II-Type III) | 0.12 | 0.09 | 0.05 |
| G_{yz} (class II-Type III) | 0.12 | 0.09 | 0.05 |

B. Interfacial Pressure Distributions

The interfacial pressure between the lower limb and ECSs was analyzed by using LS-DYNA explicit dynamics solution. When the ECS moved upward from the ankle to the knee, a depressive gradient pressure profile appeared from the ankle to

the knee. The pressure at the ankle and the knee were 2000 Pa and 800 Pa, 2500 Pa and 1000 Pa, and 3500 and 1200 Pa, respectively, for the ECSs with Classes I and II (Fig. 2).

The interfacial pressure variations related to the surface curvatures of lower limbs. The higher the curvature, the greater interfacial pressure, conversely, the lower the curvature the lower the interfacial pressure. The presence of the bones affected the distributions of transverse tissue stress. The maximum cross-sectional pressure was found at the anterior and posterior regions around the lower limb (Fig. 4).

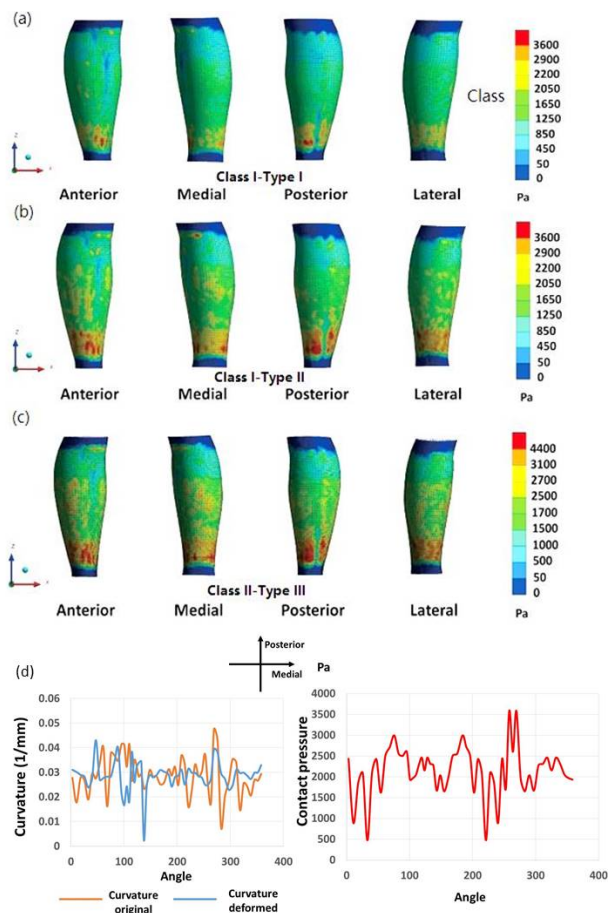


Fig. 4 Interfacial pressure exerted by (a) Class I-Type I-ECS, (b) Class I-Type II-ECS, and (c) Class II-Type-III ECS; (d) the relationship between the interfacial pressure and leg curvature exerted by Class I-Type I-ECS at the ankle.

C. Stress Transmission

The stress transmission from the skin surface to deeper tissues under pressure exertion of Class-I-Type-I ECS was computed by LS-DYNA explicit dynamics solution. The greatest stress was approximately 2000 Pa at anterior ankle, and was approximately 1300 Pa around the bones of the calf and the knee. The minimum stress was about 100 Pa between the fibula and tibia (Fig. 3). The pressure exerted on the great saphenous vein wall and small saphenous vein wall were general larger than that exerted on the peroneal vein wall.

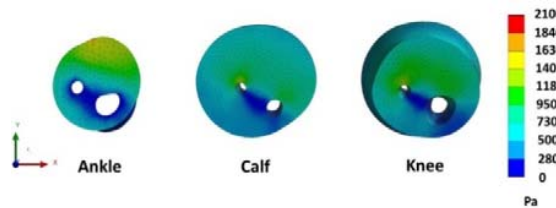


Fig. 5 Stress distribution within the cross section at the ankle, calf, and the knee by Class I-Type I ECS

D. Validation of Interfacial Pressure

The interfacial pressure between the ECSs and the lower limb were measured *in vivo* to validate the interfacial pressures distributions at ankle, calf and knee and around the anterior, posterior, medial and lateral aspects. Similar variation trends were found in the pressure magnitudes between the simulated and the measured results (Fig. 6). Larger fluctuation in pressure values occurred at the ankle and knee due to the irregularity of surface curvatures of the anatomic structures.

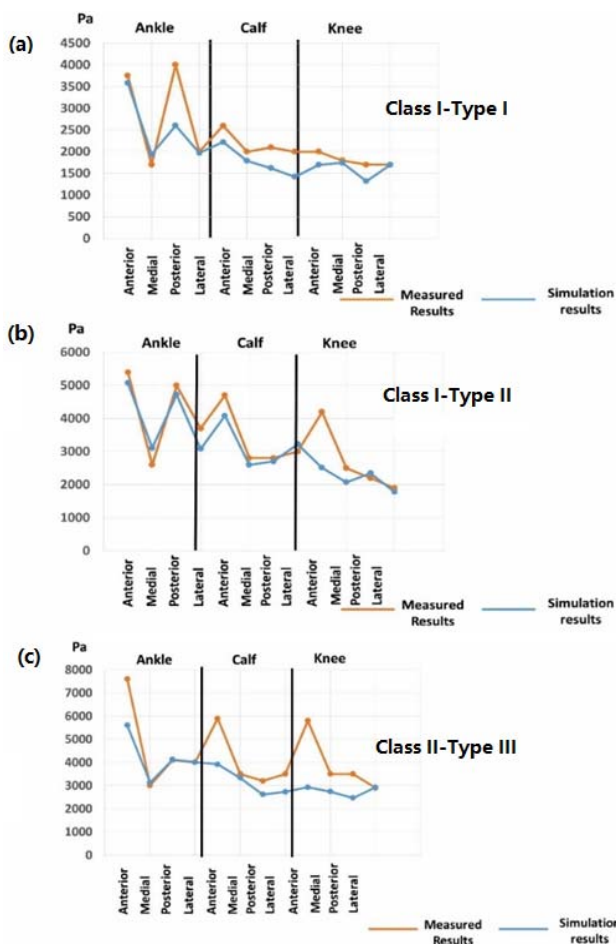


Fig. 6 Comparisons between the simulated and measured interfacial pressure for ECSs with (a) Class I-Type I, (b) Class I-Type II, and (c) Class II-Type III

E. Venous Velocity

The velocities of the studied veins under pressure action of Class I-Type I ECSs were simulated through the developed FSI coupling model. The flow velocities were increased by the intervention of the external pressure of ECS. The peak velocities of the peroneal vein, small saphenous vein, and great saphenous vein were 0.19 m/s, 0.20 m/s and 0.21 m/s at the pressure outlet, respectively (Fig. 6). Based on Poiseuille flow, the increase of the external pressure exerted on the venous walls can induce the increased flow velocity. The pressure

exerted on the venous wall was dependent on the soft tissue stress around the venous wall, indicating that the higher tissue stress could induce the increased pressure on the venous wall. As shown in Fig. 7, the peak flow velocities of the small saphenous vein and the great saphenous vein were greater than that of peroneal vein. A prediction could be made on the peak velocity of venous flow by applying Poiseuille flow, where the flow velocity was largely dependent by the tissue stress and the pressure classes of ECSs.

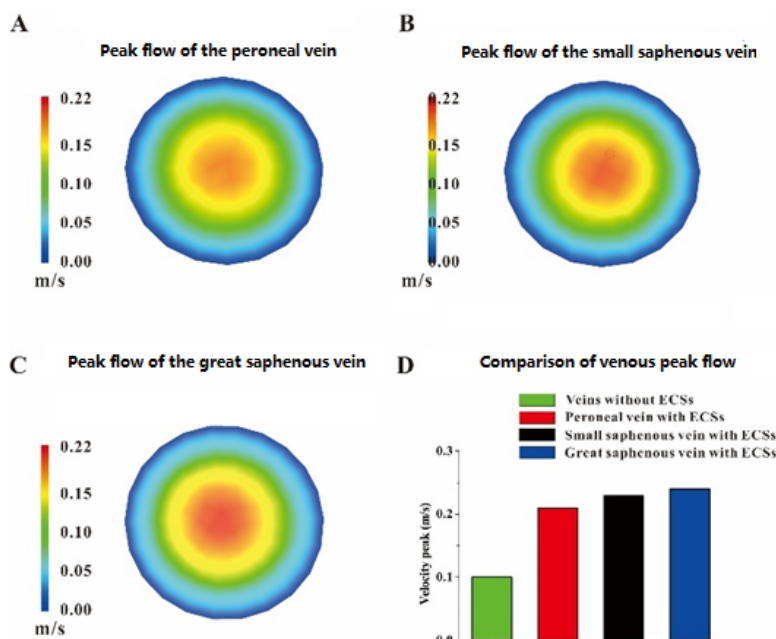


Fig. 7 Peak flow velocities at the pressure outlet, (A) the peak flow of the peroneal vein, (B) the peak flow of the small saphenous vein, (C) the peak flow of the great saphenous veins, and (D) comparison of the peak flow with and without pressure exertion by Class-I-Type I-ECS

V. CONCLUSION

The interfacial pressure, stress transmission and distribution, as well as flow velocities exerted by ECSs with different classes and mechanical properties have been objectively measured and numerically analyzed. 3D biomechanical FE model and FSI model were constructed to simulate the interfacial pressure, stress transmission, and venous flow when the ECSs were applied to the lower extremities. The simulated interfacial pressures presented a favorable agreement with the measured values, implying that the developed FE model can be applied to predict interfacial pressure and stress transmission exerted by ECSs with acceptable accuracy. Moreover, the coupled FE-FSI model contributes to predicting the interfacial pressure, stress transmission, and hemodynamics induced by ECSs, thus facilitating us to optimize structural design and material properties of ECSs to improve the efficiency of compression therapy.

ACKNOWLEDGMENT

This work was supported by the General Research Fund

(Hong Kong SAR) through project PolyU 252153/18E and Departmental General Research Fund through project G-UAHB.

REFERENCES

- [1] N Jones, R Rees, V Kakkar. A Physiological Study of Elastic Compression Stockings in Venous Disorders of the leg, *Br J Surg*67: pp. 569-572, 1980.
- [2] WRobert, DDavid. Clinical Benefits of Lightweight Compression: Reduction of Venous-Related Symptoms by Ready-to-Wear Lightweight Gradient Compression Hosiery. *DermatolSurg*,25.9, pp. 701-704. 1999.
- [3] Liu R, Guo X, Lao TT, Little TJ. A critical review on compression textiles for compression therapy: Textile-based compression interventions for chronic venous insufficiency. *Textile Research Journal*, 87(9), pp. 1121-1141, 2017.
- [4] JOLaurikka, T Sisto, M RTarkka, O Auvinen, and M Hakama,Risk Indicators for Varicose Veins in Forty-to-sixty-year-olds in the Tampere Varicose Vein Study, *World Journal of Surgery*, 26(6), pp.648, 2002.
- [5] Liu R, Lao TT, Kwok YL, Li Y, Ying M. Effects of Graduated Compression Stockings with Different Pressure Profiles on Lower-limb Venous Structures and Hemodynamics. *Advances in Therapy*, 25(5), pp. 465-478, 2008.
- [6] Liu R, Kwok YL, Li Y, Lao TT, Dai XQ, Zhang X. Numerical Simulation of Inner Stress Profiles and Deformations of Lower Extremity beneath Graduated Compression Stockings, *Fibers and Polymers*, 8(3), pp.301-308, 2007.

- [7] Liu R, Kwok YL, Li Y, Lao TT, Zhang X, Dai XQ. Objective Evaluation of Skin Pressure Distribution of Graduated Elastic Compression Stockings. *Dermatologic Surgery*, 31(6), pp. 615-624, 2005.
- [8] H Barhoumi, SMarzougui, SAbdessalem, SB Abdessalem. Clothing Pressure Modeling Using the Modified Laplace's Law, *Text Res J*, Vol.38 (2), pp.134-147,2020.
- [9] LMacintyre. Designing Pressure Garments Capable of Exerting Specific Pressures on Limbs. *Burns*, 33, pp. 579-586, 2007.
- [10] Liu R, Kwok YL, Li Y, Lao TT, Zhang X. A Three-dimensional Biomechanical Model for Numerical Simulation of Pressure Functional Performances of Graduated Compression Stocking (GCS). *Fibers and Polymers*, 7(4), pp. 389-397, 2006.
- [11] YB Shi, PLawford and R Hose, Review of Zero-D and 1-D Models of Blood Flow in the Cardiovascular System. *Biomed Eng Online*, 10.1 pp. 33, 2011.
- [12] Wakiyama, S, Takano, Y, Shiba, H, Gocho, T, Sakamoto, T, Ishida, Y, and Yanaga, K. "Significance of Portal Venous Velocity in Short-term Graft Function in Living Donor Liver Transplantation." *Transpl P* 49.5, 2017.
- [13] Ibegbuna, Veronica, Delis, Konstantinos T, Nicolaides, Andrew N, and Aina, Olayide. "Effect of Elastic Compression Stockings on Venous Hemodynamics during Walking." *J Vasc Surg* 37.2 ,2003.
- [14] Audebert, Chloe, Peeters, Geert, Segers, Patrick, Laleman, Wim, Monbaliu, Diethard, Korf, Hannelie, Trebicka, Jonel, Vignon-Clementel, Irene E, and Debbaut, Charlotte. "Closed-Loop Lumped Parameter Modeling of Hemodynamics During Cirrhogenesis in Rats." *IEEE T Cybernetics* 65.10, 2018.
- [15] L Dubuis, SAvril, JDebayle, P Badel, Identification of the Material Parameters of Soft Tissues in the Compressed Leg. *Comput Methods Biomech Biomed Engin*, 15(1), pp.3-11, 2012.
- [16] KToya, T Takahashi, Y Fujimoto, T Nishimoto, T Takasoh, K Sasano, Ken, and SKusaka, Effect of Elastic Stockings and Ankle Positions on the Blood Velocity in the Common Femoral Vein, *J PhysTherSci*, 28.9 pp.608-610, 2016.

Chongyang Ye, a current PhD student, the Hong Kong Polytechnic University, received MSc degree from Beijing University of Technology (2017) and Bachelor degree from Shenyang Aerospace University (2013). His research work relates to FEM biomechanical analysis. His related publications include "Novel Cone-and-plate Flow Chamber with Controlled Distribution of Wall Fluid Shear Stress" (CY Ye, et al) in *Computers in Biology and Medicine* (2019), and "Migration and Differentiation of Osteoclast Precursors under Gradient Fluid Shear Stress" in *Biomechanics and Modeling in Mechanobiology* (2019).

Rong Liu, Assistant Professor, Institute of Textiles and Clothing, The Hong Kong Polytechnic University. She holds PhD degree in Textiles and Clothing Science and Technology, and MSc degrees in Biomedical Engineering and Clothing Engineering. She ever worked as Research Fellow in Rehabilitation Sciences, and Visiting Assistant Professor of College of Textiles, North Carolina State University. Her research interests include functional compression textiles, clothing biomechanics, and textiles/apparel innovation for healthcare and medical treatment.